Journal of Fluid Science and Technology

Vol. 4, No. 3, 2009

Numerical Simulation of Bypass Transition by the Approach of Intermittency Transport Equation*

Most. Nasrin AKHTER**, Kazutoyo YAMADA*** and Ken-ichi FUNAZAKI***

**Graduate School of Iwate University

4-3-5, Ueda, Morioka, Iwate 020-8551, Japan

*** Department of Mechanical Engineering, Iwate University

4-3-5, Ueda, Morioka, Iwate 020-8551, Japan

E-mail: funazaki@iwate-u.ac.jp

Abstract

This paper deals with the development of a numerical approach to predict freestream turbulence-induced (FST-induced) boundary layer bypass transition using an intermittency transport equation. An intermittency based transition model, which is critical for invoking transition onset according to Abu-Ghannam and Shaw correlation, is implemented into the proven Reynolds-Averaged N-S (RANS) solver. The intermittent behavior of the transitional flow is incorporated into the computation by modifying the eddy viscosity μ_t, obtained from a turbulence model. Wilcox low Reynolds $k-\omega$ turbulence model is employed to calculate the eddy viscosity and others turbulent quantities. For validation, the present transition model is applied to the benchmark experiments of flat plate test cases of ERCOFTAC series and to predictions of a modern Low Pressure (LP) turbine flow. It follows from the detail comparisons of the calculated results with the relevant experimental data and other researchers' simulations that the present model is capable to make a reasonable prediction of FST-induced bypass transition.

Key words: Boundary Layer, Bypass Transition, Numerical Prediction, Intermittency Factor

1. Introduction

The process in which a laminar boundary layer changes to a turbulent boundary layer is termed boundary layer transition. Since heat transfer and skin friction tend to increase dramatically throughout the transitional region, accurate prediction of this process is of practical importance in gas turbine industries. At this moments, unfortunately, the boundary layer transition is still a very difficult phenomenon to make a full understanding of and will stay as a long-lasting challenging problem. This is because the boundary layer transition is easily influenced by various kind of factors such as freestream turbulence, wake passing or surface roughness. It is a widely accepted idea that the transition governed by the freestream turbulence or wake passing, which is called bypass transition, is a common mode of boundary layer transition in gas turbines. Therefore accurate prediction of bypass transition induced by freestream turbulence, which can be called FST-induced bypass transition, is important but challenging task for developing reliable and highly efficient gas turbines.

As the turbulence modeling makes steady progresses over the years, FST-induced transition can be simulated to some extent nowadays, usually using RANS (Reynolds-Averaged Navier-Stokes equations) based approach with low Reynolds version of two equation model. However such a prediction tended to predict too early transition onset and/or too fast completion of the transition in comparison with the measurements, even for the simple flat plate case. One example of the seemingly successful approaches to predict FST-induced transition was that of Schmidt and Patankar[1] using Production Term Modification method. Their method aimed at control of the evolution process of

*Received 9 Jan., 2009 (No. 09-0014)
[DOI: 10.1299/jfst.4.524]

turbulent kinetic energy in order to emulate realistic transitional behaviors of the boundary layer. Unfortunately, the approach of Schmidt and Patankar failed to gain popularity even among the turbomechinary community, probably because it requires two empirical parameters in a first-order ordinary differential equation that does not have any physical meaning, along with the difficulty in implementing their method into N-S solvers.

An alternative approach for predicting the bypass transition, which is nowadays being implemented into some of the commercial codes, is the usage of intermittency[2)-6)]. The concept of intermittency, a measure of the probability of a given point to be inside the turbulent region, has evolved from the need to distinguish between ordered and random behaviors of the flow in the intermittent region. Recently Suzen and Huang[7] proposed a sophisticated intermittency-based transition model by combining two intermittency equations (Stellant and Dick[3] and Cho and Chung[4] model). Their transition model has turned out to be superior to the precedents in predicting the bypass transition, however, some test cases identified that there still remained some discrepancies between the prediction and experimental data, in particular for high freestream turbulence cases (such as around 10%) that are commonly observed in the flow field of gas tubines[17]. Very recently the present authors (Akhter and Funazaki[8]) introduced a new intermittency based transition model, using Schmidt and Patankar[1] boundary layer analysis code. Their model exhibited a comparable or in some cases better predicting capability in terms of accuracy for wide range of freestream turbulence intensity than Suzen – Huang model.

The present study then tries to apply the same approach as that adopted in the previous boundary layer analysis code[8] to a well-established highly accurate RANS code. Some adjustment should be made on the intermittency transport equation since this code employs Wilcox $k-\omega$ model. The newly developed code is tuned and tested against T3 series of experiments of Savill[10]and prediction of the $k-\varepsilon-\gamma$ model of Suzen and Huang[7] $k-\varepsilon$ model of Launder-Sharma[13] and the base model of Wilcox[9] $k-\omega$. Then the code is applied to rather a challenging problem, that is the prediction of flow field around the LP turbine airfoil that was extensively investigated by Simon et al.[17].

Nomenclature

C_f : skin friction coefficient
c_{gi} : empirical contants for intermittency transport equation
C_μ : model constant for eddy viscosity
H_{12} : shape factor ($=\delta^*/\theta$)
C_p : pressure coefficient
K : acceleration parameter
k : turbulent kinetic energy
P_k : production of turbulent kinetic energy
L_x : axial chord length
L_{ss} : suction surface length
Re : Reynolds number, $L_{ss}U_{exit}/\nu$
Re_x : Reynolds number based on x
Re_θ : Reynolds number based on momentum thickness
s : streamwise distance along the surface from the stagnation point
p : static pressure
p_{total} : total pressure
Tu : turbulence intensity
U_e : freestream velocity
U_{in} : inlet velocity
U_{exit} : exit velocity
U : streamwise velocity component
x : surface length from the leading edge
y : distance normal to the wall
y^+ : non-dimensional distance from the wall
γ : intermittency factor
δ : momentum boundary layer thickness

δ_t : thermal boundary layer thickness
ε : dissipation rate
δ^* : displacement thickness
θ : momentum thickness
μ : moleculer viscosity
μ_t : eddy viscosity
ρ : density

Subscripts

e : freestream
tr : transition onset

2. New Transition Model

RANS-based intermittency transport equation (abbreviated as ITE) is developed as shown in the following by modifying Cho and Chung[4] model. The aim of this modification is to improve the capability of the original model for predicting transition of wall bounded shear flows and at the same time to raise the reproductivity of the intermittency profile in the cross stream direction. The proposed transport equation is coupled with Wilcox low Reynolds $k-\omega$ model[9] with no modification.

2.1 Intermittency (γ) equation

The proposed intermittency equation is

$$\frac{\partial}{\partial t}(\rho\gamma)+\frac{\partial}{\partial x_j}(\rho u_j\gamma)=c_{g_1}\gamma(1-\gamma)\frac{P_k}{k}+\frac{c_{g2}}{\beta^*}\rho\frac{k}{\omega}\frac{\partial\gamma}{\partial x_j}\frac{\partial\gamma}{\partial x_j}+\frac{\partial}{\partial x_j}\left[\sigma_\gamma(1-\gamma)(\mu+\mu_t)\frac{\partial\gamma}{\partial x_j}\right] \quad (1)$$

The first term of right hand side represents the production term, where $P_k=2\mu_t' S^2$ represents the production of turbulent kinetic energy by the shear stress, where $\mu_t'=k/\omega$. This term expresses the generation of γ owing to the production of the turbulent kinetic energy. The second term represents the increase of γ by the spatial inhomogeneity or gradient of γ itself. The last term represents the diffusion term. The role of diffusion term is to allow a gradual variation of γ towards zero in the freestream.

Here presented intermittency transport equation is coupled with the turbulent kinetic energy k and its dissipation ω equation, whereas the original Cho and Chung[4] model was coupled with the equations of turbulent kinetic energy and its dissipation rate ε. The conversion of ITE from $k-\varepsilon$ model to $k-\omega$ model was made simply using $\varepsilon=\beta^*\omega k$, where $\beta^*=0.09$. Details will appear in the following.

The present model also differs from the original version of Cho and Chung[4] in diffusion term and empirical constants. The proposed new diffusion term is expected to induce gradual increase of intermittency in the streamwise direction with the newly selected set of model constants tuned for wall bounded shear flows. Note that the original model constants were selected based only on plane jet experiments. Since any sink term does not exist in the original model of Cho and Chung, the destruction effect is embodied by decreasing the model constant C_{g1}, which controls overall transitional behavior. In the present model the value of C_{g1} is set to be 0.19 based on the previous finding by the authors[8], where the original constant was 1.6. The model constant C_{g2} is set to be 1.0 instead of original constant 0.15. As shown later, this constant affects the transition lengths in higher turbulence intensity cases, and its value was finally determined through numerical experiments[20] so as to achieve reasonable agreement with the measured data for the wide range of turbulence intensity. We have dropped the entrainment effect as this effect is found to be negligible for most flows.

The intermittency concept was incorporated in to the computation through the eddy viscosity. The eddy viscosity relation then modifies

$$\nu^*_t=\nu_t\left[1+C_{\mu g}\frac{k}{\omega^2}\gamma^{-2}(1-\gamma)\frac{\partial\gamma}{\partial x_k}\frac{\partial\gamma}{\partial x_k}\right] \quad (2)$$

The above expression for the eddy viscosity was originally proposed by Cho and Chung[4] to account for the effect of outer irrotational fluid motion. The above relation Eq.(2) reduces to the fully turbulent flow when $\gamma = 1.0$. Eddy viscosity ν_t is calculated from the Wilcox low Reynolds $k-\omega$ model in the present model. Finally the model empirical constants adopted are

$$c_{\mu g} = 0.001 \quad c_{g1} = 0.19 \quad c_{g2} = 1.0 \quad \sigma_\gamma = 1.0 \tag{3}$$

2.2 Baseline turbulence model and onset location.

As mentioned above, the two equation $k-\omega$ turbulence model of Wilcox[9] was chosen. The model reads as follows,
Turbulent Kinetic energy (k)

$$\frac{\partial}{\partial t}(\rho k) + \frac{\partial}{\partial x_j}(\rho u_j k) = \tau_{ij}\frac{\partial u_i}{\partial x_j} - \beta^* \rho\omega k + \frac{\partial}{\partial x_j}\left[(\mu + \sigma^* \mu_T)\frac{\partial k}{\partial x_j}\right], \tag{4}$$

Specific dissipation rate of turbulent kinetic energy (ω)

$$\frac{\partial}{\partial t}(\rho\omega) + \frac{\partial}{\partial x_j}(\rho u_j \omega) = \alpha\frac{\omega}{k}\tau_{ij}\frac{\partial u_i}{\partial x_j} - \beta\rho\omega^2 + \frac{\partial}{\partial x_j}\left[(\mu + \sigma\mu_T)\frac{\partial \omega}{\partial x_j}\right], \tag{5}$$

And eddy viscosity,

$$\nu_t = \alpha^* \frac{k}{\omega} \tag{6} \qquad \alpha^* = \frac{\alpha_0^* + Re_t/R_k}{1 + Re_t/R_k}, \quad Re_t = \frac{\rho k}{\mu\omega} \tag{7}$$

$$\alpha = \frac{5}{9}\frac{\alpha_0 + Re_t/R_\omega}{1 + Re_t/R_\omega}(\alpha^*)^{-1} \tag{8} \qquad \beta^* = \frac{9}{100}\frac{5/18 + (Re_t/R_\beta)^4}{1 + (Re_t/R_\beta)^4} \tag{9}$$

The empirical constants of the Wilcox model are

$$\beta = \frac{3}{40}, \quad \sigma^* = \sigma = 0.5, \quad \alpha_0^* = \frac{\beta}{3}, \quad \alpha_0 = 0.1, \quad R_k = 6, \quad R_\omega = 2.7, \quad R_\beta = 8 \tag{10}$$

One of the important points associated with transition prediction using the intermittency-based turbulence model is to specify the transition onset point properly since the intermittency transport equation does not feature a capability to tell where the transition will occur. This study has employed the well known Abu-Ghannam and Shaw[12] correlation for determining onset location, which is given as follows;

$$Re_{\theta_t} = 163 + \exp(6.91 - Tu), \tag{11}$$

where Tu is turbulence intensity at a reference point and Re_θ is the Reynolds number based on momentum thickness at onset location. Before the onset location, the production term of turbulent kinetic energy was set to be zero inside the boundary layer.

2.3 Numerical Method

Calculations have been done by the CFD code developed by Yamada et al[19]. The three dimensional Reynolds averaged Navier-Stokes equations are discretized spatially by a cell-centered finite volume formulation and in time using the Euler implicit method. The inviscid fluxes at cell interfaces are evaluated using a highly accurate upwind scheme based on a TVD formulation (Furukawa et.al[16]), where a Roe's approximate Riemann solver of Chakravarthy[15] and third order accurate MUSCL-type approach with the Van Albada limiter were implemented. The viscous fluxes are determined in a central differencing manner with Gauss's theorem. Simultaneous equations linearized in time were solved by a point Gauss-Seidel relaxation method. The code is able to deal with the multi-blocked computational grid system taking advantage of MPI.

3. Results and Discussion

Two types of calculations have been made in this paper to check the validity of the proposed intermittency model. The first calculation dealt with flat plate test cases with zero pressure gradient,

using geometrical and experimental data taken from the existing experiment known as ERCOFTAC so called T3 series (Savill[10]). Those data are frequently used as a benchmark for validating any transition model. The second calculation examined the flow field through a low pressure turbine cascade called PAK-B, employing the cascade configuration and the experimental data from the study done by Simon et. al.[17]. This experiment covered the wide range of Reynolds numbers and FSTI values and it offers a good test case for investigating influences of freestream turbulence intensity and Reynolds number upon the bypass transition.

3.1 Test Cases of Flat plate

In T3 series the first two cases (T3A, T3B) are for zero pressure gradient with freestream turbulence intensity (FSTI) 3% and 6%, respectively. The grid sensitivity study was first performed for each of the simulations. Grid sensitivity was checked by using four types of grids and $100\times100\times4$ was finally chosen, where the streamwise grid point number was 100 and crosstream grid point number was also 100. The streamwise direction grid was clustered around the leading edge. The grid was expanded in crossstream direction with the first wall unit grid spacing y^+ approximately equal to unity. The grid configuration of the plate is shown in Figure 1.

In all computation, the inlet turbulent kinetic energy was fixed at the experimental freestream turbulence level. The onset of transition was specified according to the correlation of Abu-Ghannam and Shaw[12] for all cases. Comparisons are performed for these cases among the relevant experimental data and the predictions using the new transition model, conventional turbulence models of Launder –Sharma $k-\varepsilon$ model[13], $k-\omega$ model of Wilcox[9] and Suzen-Huang $k-\varepsilon-\gamma$ model[7].

Figure 2 shows the surface skin friction coefficients C_f for T3A case. As can be seen in Figure 2, Launder-Sharma $k-\varepsilon$ model and Wilcox $k-\omega$ model predicted early transition, while Suzen-Huang $k-\varepsilon-\gamma$ model and the present model exhibited better performance in the prediction of the skin friction coefficients. It appears that the present model yielded an improved agreement with the experiment in comparison with that of the Suzen-Huang model.

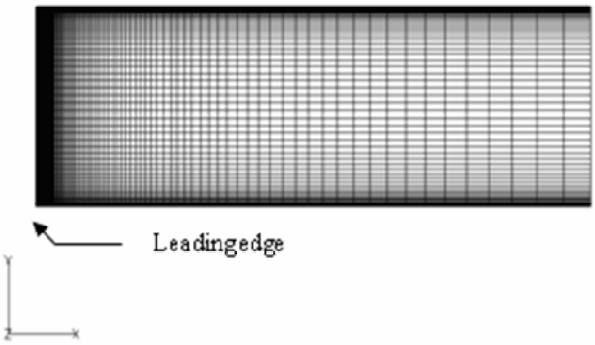

Figure 1 Grid system used for flat plate simulations

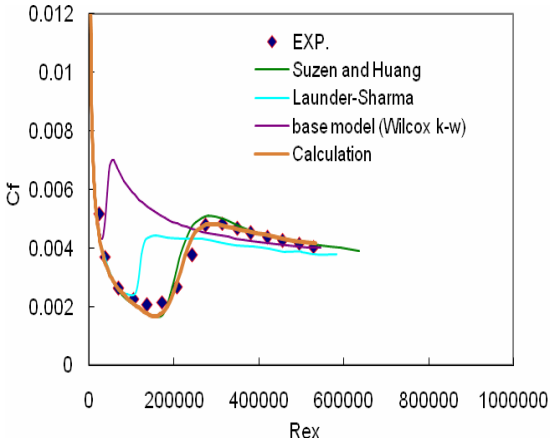

Figure 2 Comparison of surface skin friction coefficient for T3A case

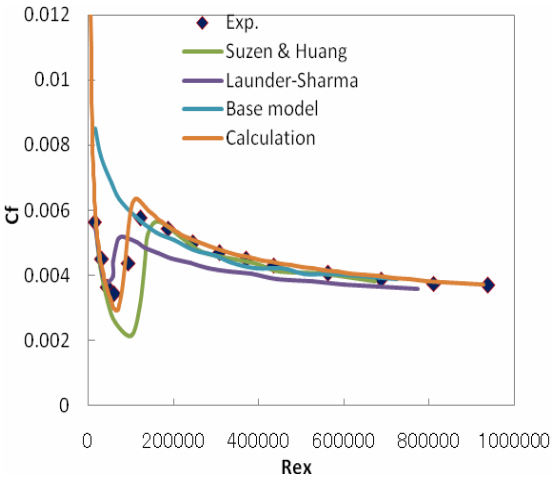

Figure 3 Comparison of surface skin friction coefficient for T3B case

The second test case of T3 series is the T3B case. This test case is also for flat plates zero pressure gradient flow with freestream turbulence intensity 6 % at the leading edge. Due to this higher freestream turbulence intensity, the boundary layer experienced very early transition. Figure3 clearly demonstrates that the prediction by the present model matched the experimental skin friction coefficient more adequately than any other models employed in this study. Again the Wilcox model and Launder-Sharma model yielded much prompted transition and the model of Suzen and Huang predicted slightly delayed onset of transition.

3.2 Test Cases of LP Turbine blade

The intermittency transport model was been applied to the low pressure turbine blade of Pratt and Whitney (Pak-B blade). Measurement were made on the suction surface of the blade at locations from P2 to P13 as shown in Figure 4. Note that the exact positions in terms of the suction surface length are as follows: location 2; 4.5%, location 3; 17.8%, location 4; 29%, location 5; 35%, location 6; 40.9%, location 7; 47%, location 8; 52.9%, location 9; 59%, location 10; 67.9%, location 11; 73.8%, location 12; 82.1%, and location 13; 92.6%.

These experiments were conducted in order to examine the effect of Reynolds numbers and freestream turbulence intensity. Four Reynolds number; Re= 50,000, 100,000, 200,000, 300,000 and three levels of freestream turbulence intensity, 0.5%, 2.5%, 10% were studied. The Reynolds number was based upon the exit velocity and suction surface length. The calculations were performed with H type of grid with inlet and outlet boundaries set one chord length upstream and downstream of the turbine blade leading and trailing edges, respectively. No slip boundary condition was applied to the blade surface and periodic boundary condition was applied along with the pitch wise direction. The wall unit y^+ of the nearest grid point to the blade surface was approximately equal to 0.5. The grid dependency study was first performed in a linear cascade and the sensitivity was checked. As a result all calculations reported here were obtained by the use of grid $400\times4\times100$ where the surface grid point number was 200 along stream wise direction and cross-stream wise grid point number was 100.
In the present study two freestream turbulence intensity (FSTI=10% and =2.5%) and three Reynolds number were dealt with. For the FSTI=10% case the Reynolds number examined were $Re=1\times10^5$ and $Re=2\times10^5$ and for the case FSTI=2.5% the Reynolds numbers were $Re=2\times10^5$ and $Re=3\times10^5$. Figure 5 shows the comparisons of pressure coefficients over the blade suction surface for $Re=2\times10^5$ and $Re=3\times10^5$ with FSTI=2.5%. Actually in this case inlet turbulence intensity was set to 3% at the inlet boundary, which eventually decayed so as to become 2.5% near the blade leading edge. Transition onset location was determined by setting Tu=2.5% in Eq. (11). Agreement between the calculations and the experiment was good, where the coefficient was defined as

$$C_p = (p_{total} - p) / \frac{1}{2}\rho U_{exit}^2 . \quad (12)$$

As shown in Figure 5(a), the measurement for $Re = 2\times10^5$ indicates the existence of separation and reattachment around x / L_x =0.7-0.8. The corresponding calculation reasonably reproduced those phenomena. For higher Reynolds number case, i.e. $Re = 3\times10^5$ it is clear that the separation was substantially suppressed.

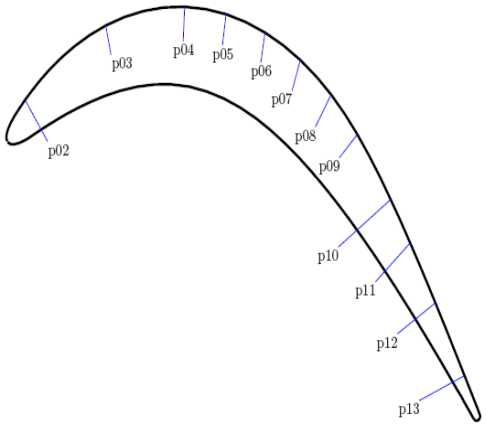

Figure 4 Pak-B airfoil geometry and measurement stations on the suction surface of the blade

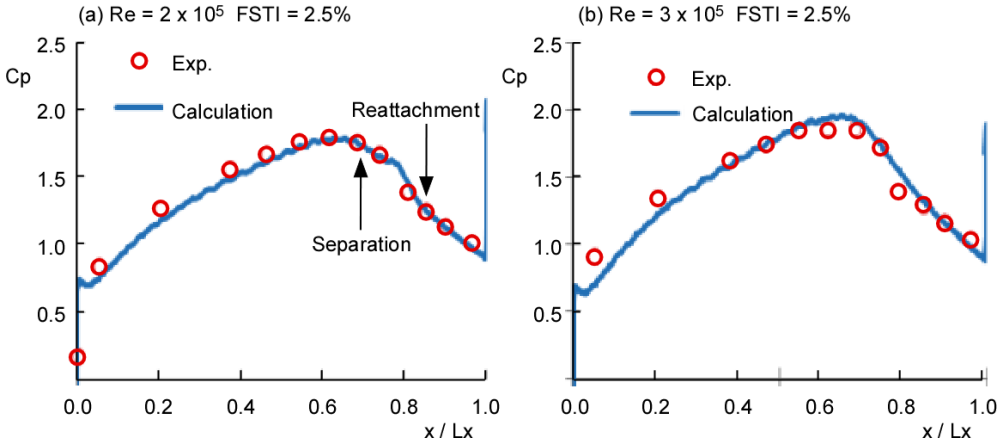

Figure 5 Comparisons of pressure coefficient for the cases of (a) $Re = 2\times10^5$ and FSTI=2.5% (b) $Re = 3\times10^5$ and FSTI=2.5% .

Figure 6 shows calculated and measured velocity profiles for the case of FSTI 2.5% and $Re = 2\times10^5$. It seems from the comparison that the velocity profiles calculated in this study agree with the measurements on the upstream portion (p02-p07). From the comparisons of the data on the aft portion (p08-p13), reasonable prediction of separation bubble was observed. Note that Suzen and Huang model showed little earlier reattachment of the separation bubble at position p10, while the present model almost reproduced the experiment. Unfortunately, the present model failed to capture the transitional behavior of the separation bubble, which can be attributed to the lack of a function in the model to invoke separation induced transition. The present authors are now underway to cope with this task. The next case was FSTI=2.5% and $Re = 3\times10^5$, as shown in Figure 7. The comparison of velocity profile in the front portion of the blade shows that good agreement was observed over the region from p02-p07. The experiment also suggested that there appeared a separated region around p09 station, which was so tiny that not only the present model but also Suzen and Huang model did not reproduce the reverse flow.

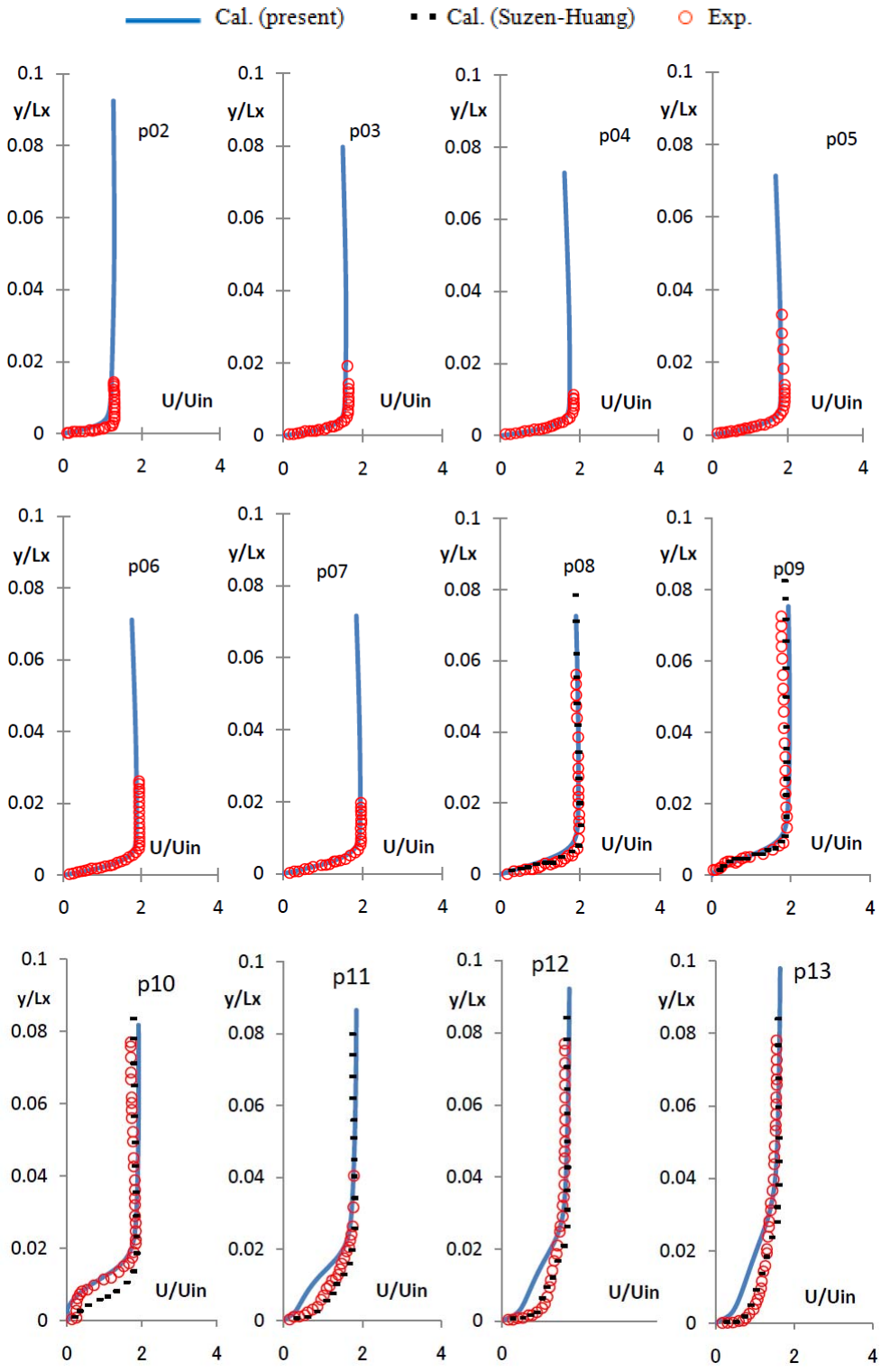

Figure 6 Comparisons of velocity profile from p02-p13, for the case of $Re = 2 \times 10^5$ and FSTI=2.5%

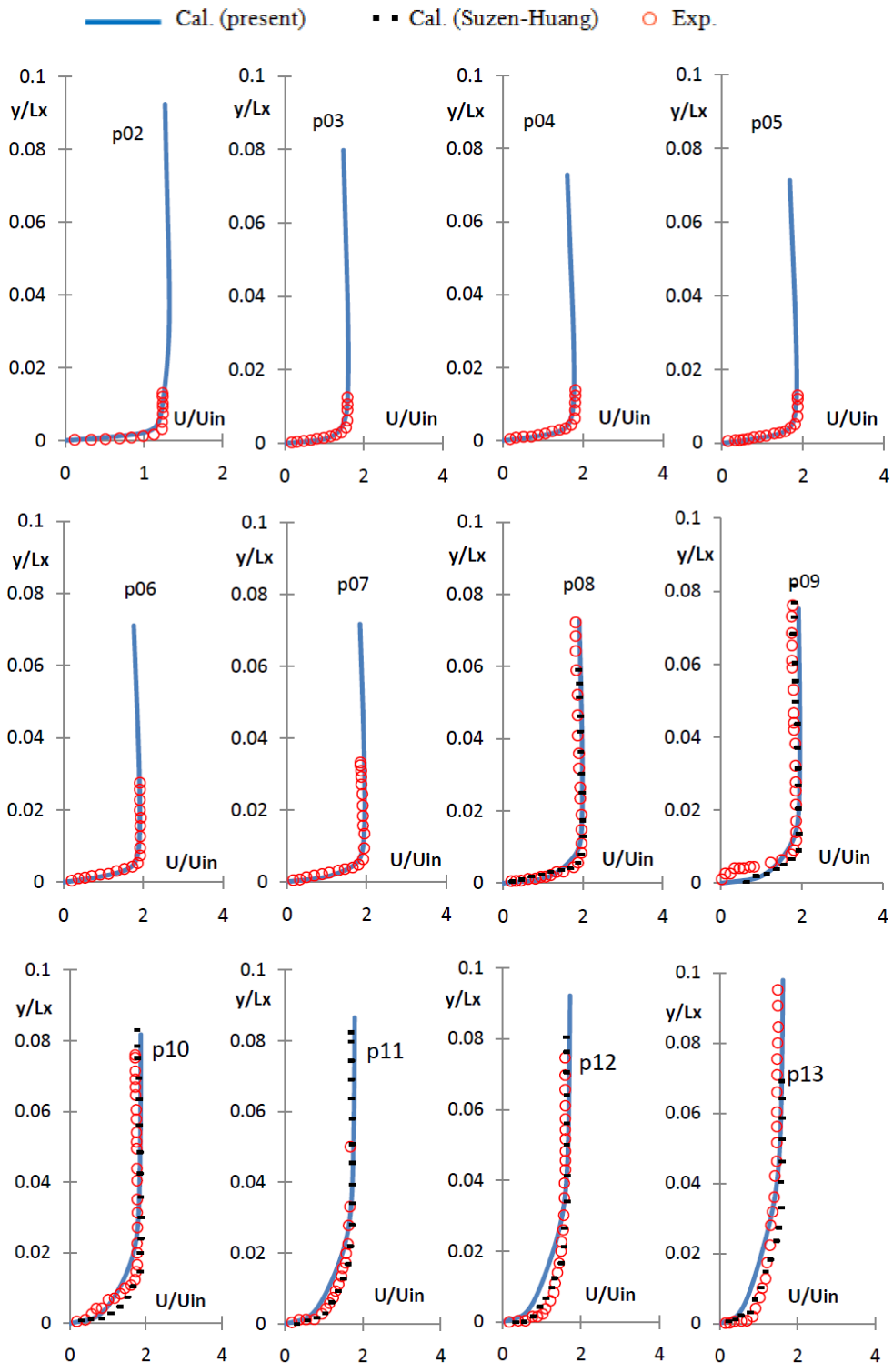

Figure 7 Comparisons of velocity profile from p02-p13, for the case of $Re = 3 \times 10^5$ and FSTI=2.5%

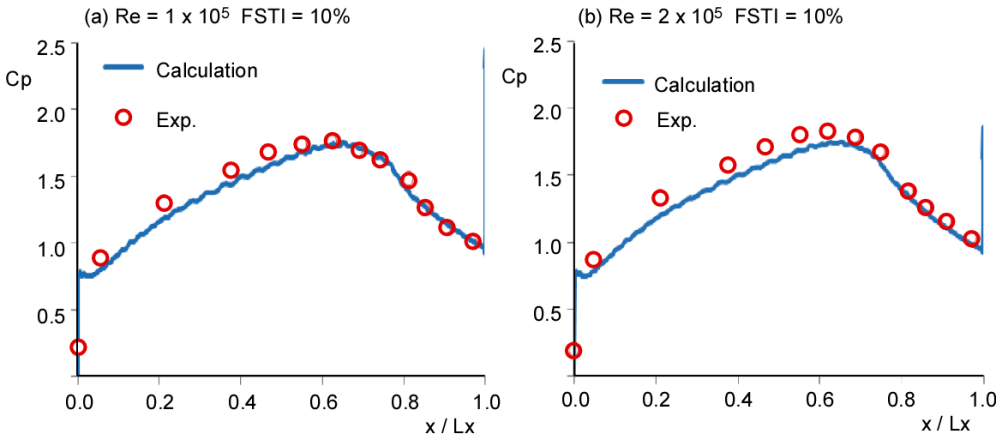

Figure 8 Comparison of pressure coefficient for the case of (a) $Re = 1 \times 10^5$ **and FSTI=10% (b)** $Re = 2 \times 10^5$ **and FSTI=10%**

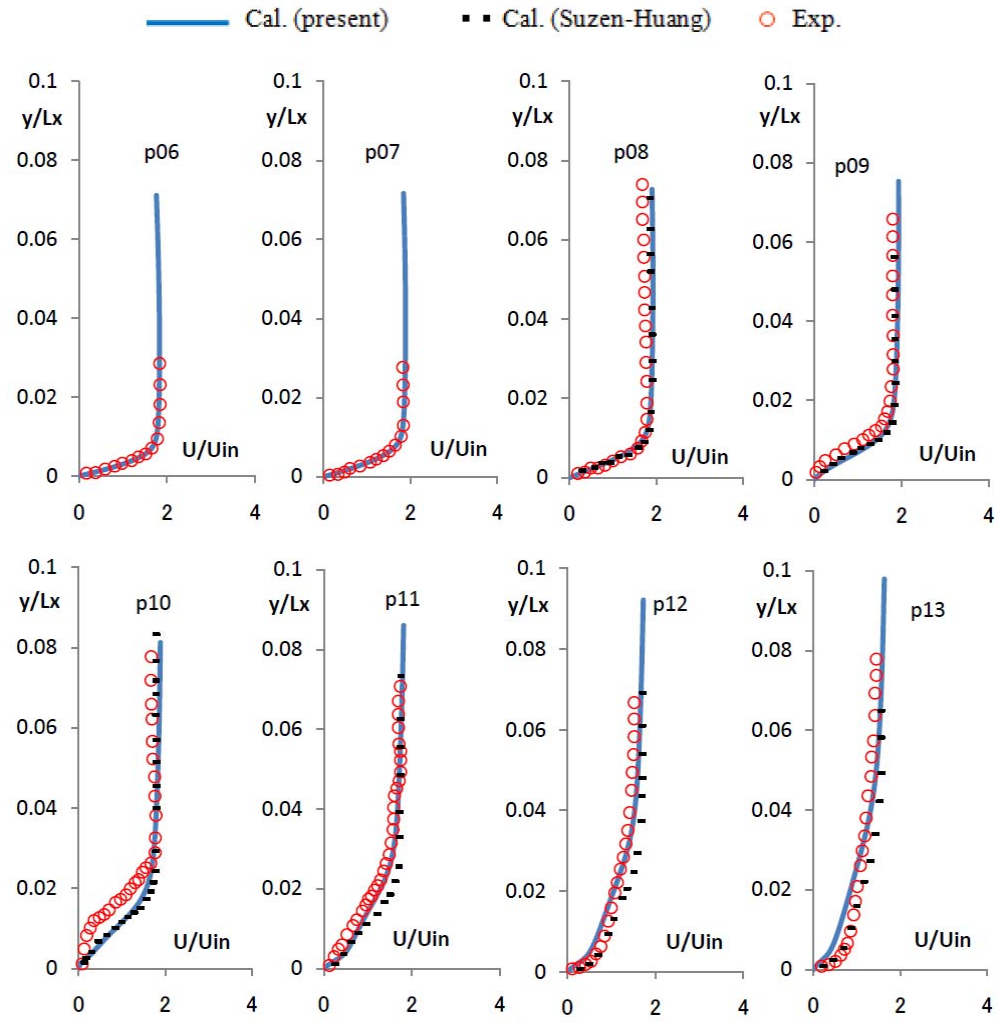

Figure 9 Comparison of velocity profile from p06-p13, for the case of $Re = 1 \times 10^5$ **and FSTI=10%**

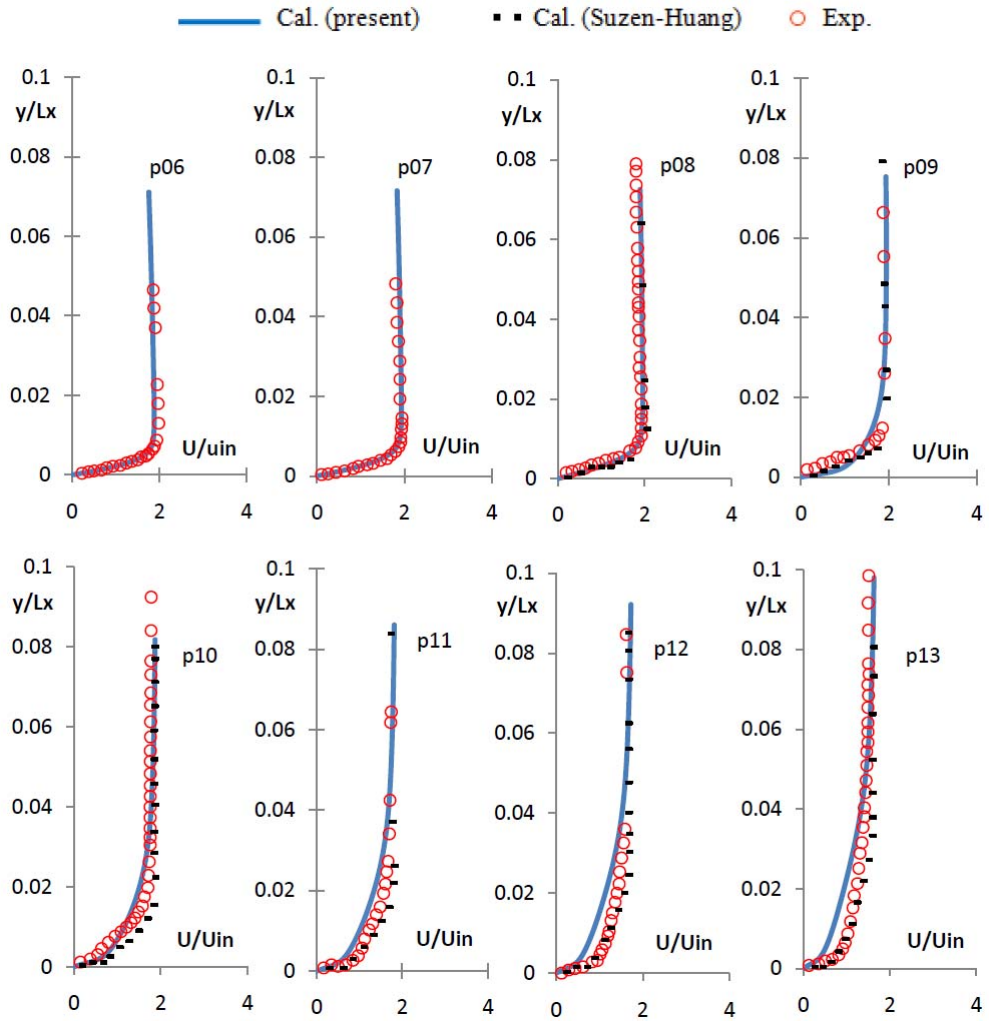

Figure 10 Comparison of velocity profile from p06-p13, for the case of $Re = 2 \times 10^5$ and FSTI=10%

Figure 8 shows the comparison of pressure coefficients over the blade suction surface for $Re = 1 \times 10^5$ and $Re = 2 \times 10^5$ with FSTI=10%. These are the highest turbulence intensity cases dealt with in this study. This high level of freestream turbulence intensity caused earlier transition than the lower turbulence intensity case. In both cases onset of transition was determined by the local freestream turbulence intensity. As shown in Figure 8(a), although this was the highest FSTI case, the flow had a separation zone again over p09-p10 stations due to its low Reynolds number. The corresponding calculation reasonably reproduced those phenomena. For higher Reynolds number, i.e. $Re = 2 \times 10^5$ it is clear that the separation was substantially suppressed.

Detail comparisons of velocity profile for the case of $Re = 1 \times 10^5$ and FSTI=10% are shown in Figure 9, where the present model and Suzen and Huang model captured the features of all velocity profiles fairly well, except p10 station. The next case is for turbulence intensity 10% and Reynolds number $Re = 2 \times 10^5$. As the Reynolds number increased, the boundary layer experienced early transition and separation bubble was seemingly suppressed, although the experiment suggested there remained a very tiny separation. As the separation was very tiny, there was virtually no reverse flow. The velocity profiles for this case are shown in Figure 10. Good agreement was again obtained over the all measurement locations. Compared to Suzen and Huang model, the present model captured the reattachment occurring around p10 fairly well.

4. Concluding Remarks

A transition model, based on a dynamic transport equation for the intermittency factor, has been

presented with some improvements especially of prediction accuracy for high freestream turbulence cases that are commonly found in gas turbines. For validation, the new model was tested against cases of transitional boundary layer on the flat plate with zero pressure gradient as well as transitional boundary layer of low pressure turbine accompanied with separation bubble. In all flat plate cases the model showed good agreement with the experiments. On the other hand, since the low pressure turbine cascade cases were tough test cases for the present model due to the co-existence of attached and separated boundary layer transition modes, some discrepancies were observed between the predictions and the measurements. However, as a whole, the present approach seems promising and worthy of being implemented in the various types of RANS codes. Still, further study is to be continued to improve capability of the present model by applying it to various kinds of flow fields.

References

(1) Schmidt, R. C., and Patanker, S. V., Two-Equation Low-Reynolds –Number Turbulence Modeling of Transitional Boundary Layer Flows Characteristic of Gas turbine Blades, *NASA Contractor Report* 4145 (1988).
(2) Dhawan, S., and Narasimha, R., Some Properties of boundary Layer during the transition from laminar to turbulent flow motion, *Journal of Fluid Mechanics*, Vol. 3 (1958) , pp. 418-436
(3) Steelant, J., and Dick, E., Modelling of bypass transition with conditioned NS equations coupled to an intermittency transport equation, *International Journal for Numerical Methods in Fluids.* Vol. 23 (1996), pp. 193-220.
(4) Cho, J. R., and Chung, M. K., A $k-\varepsilon-\gamma$ Equation Turbulence Model, *Journal of Fluid Mechanics,* Vol. 237 (1992), pp. 301-322
(5) Myong H. K. and Kasagi N., A new proposal for a $k-\varepsilon$ turbulence model and its evaluation, *Transaction of JSME(B),* Vol.54 (1988), pp. 3003-3009
(6) Libby, P. A., On the prediction of intermittent turbulent flows, *Journal of Fluid Mechanics*, Vol. 68, part 2 (1975), pp. 273-295.
(7) Suzen, Y. B., and Huang, P. G., Modelling of flow transition using an intermittency transport equation for modeling flow transition, *Journal of Fluid Engineering*. Vol.122 (2000), pp.273-284
(8) Akhter, M.N., Funazaki, K., Development of Prediction Method of Boundary Layer Bypass Transition using Intermittency Transport Equation, *International Journal of Gas Turbine, Propulsion and Power Systems*, Vol. 1 (2007), pp 30-37.
(9) Wilcox, D. C., Simulation of Transition with a Two-Equation Turbulence Model, *AIAA Journal.,* Vol.32, No.2 (1994), pp. 247-255
(10) Savill, A. M., Further progress in the turbulence modeling of bypass transition, Engineering Turbulence Modeling and Experiments 2, W. Rodi and F. Martelli, Eds., *Elsevier science*, (1993), p. 583-592
(11) Byggstoyl and Kollmann, W., A closer models for conditioned stress equations and its application to turbulent shear flows, *Physics of Fluids* Vol. 29 (1986), 1430
(12) Abu-Ghannam, B. J., and Shaw, R., Natural transition of boundary layer the effect of turbulent pressure gradient and flow history, *Journal of Mechanical Scienece,* Vol.22, No.5, (1980), pp. 213-228
(13) Launder, B. E., and Sharma, B. I, Application of the energy dissipation model of turbulence to the calculation of flow near a Spinning Disc, *Letters in Heat and Mass Transfer,* Vol. 1, (1974), pp. 131-138
(14) Anderson, W. K., Thomas, J. L., and Van Leer, B., Comparison of Finite Volume Flux Splitting for the Euler Equation, *AIAA Journal*, Vol.24, No.9, (1986), pp. 1453-1460
(15) Chakravarthy, S. R., The Versatility and Reliability of Euler Solvers Based on High –Accuracy TVD Formulations, AIAA paper No. 86-0243, (1986).
(16) Furukawa, M., Yamasaki, M., and Inoue, M., A Zonal approach for Navier-stokes Computations of Compressible Cascade Flow Fields Using a TVD Finite Volume Method, *ASME Journal of Turbomechinary*, Vol.113 No.4, (1991), pp. 573-582.
(17) Simon, T. W., Qiu, S., and Yuan, K., Measurement in a Transitional Boundary Layer Under Low-Pressure Turbine Airfoil Conditions, NASA CR 2000-209957, (2000)
(18) Suzen, Y.B., Xiong, G., and Huang, P.G., " Predictions of Transitional Flow in Low-Pressure Turbines Using Intermittency Transport Equation," *AIAA Journal*, Vol. 40, No. 2, (2002), pp. 254-266.
(19) Yamada, K., Furukawa, M., Nakano, T., Inoue, M., Funazaki, K., "Unsteady Three-Dimensional Flow Phenomena Due to breakdown of Tip Leakage Vortex in a Transonic Axial Compressor Rotor," ASME Paper, GT 2004-53745, (2004).
(20) Akhter, M.N., "Deveropment of Boundary Layer Bypass Transition Prediction Methods Based on Intermittence Factor," Doctoral Dissertation, Iwate University, (2008).